

LNF-76/8(R)

16 Febbraio 1976

G. Bologna, R. Bonini, G. Catitti, B. D'Ettorre Piazzoli, F. L. Fabbri, M. Giardoni, G. Mannocchi, E. Montanari, M. Pallotta, P. Picchi, D. Pistoni, G. Rivellini, L. Satta, P. Spillantini, D. Traverso, G. Ubaldini and A. Zallo: CONSTRUCTION AND TESTING OF A LIGHT CYLINDRICAL MULTIWIRE PROPORTIONAL CHAMBER PROTOTYPE.

G. Bologna, R. Bonini, G. Catitti, B. D'Ettore Piazzoli^(x), F. L. Fabbri, M. Giardoni, G. Mannocchi^(x), E. Montanari, M. Pallotta, P. Picchi, D. Pistoni, G. Rivellini, L. Satta, P. Spillantini, D. Traverso, G. Ubaldini and A. Zallo: CONSTRUCTION AND TESTING OF A LIGHT CYLINDRICAL MULTIWIRE PROPORTIONAL CHAMBER PROTOTYPE. -

ABSTRACT. -

We describe the construction technique and the performances of a multiwire proportional chamber prototype, which will be placed in the central core of the vertex detector of the FRAMM experiment (Frascati - Pisa-Roma collaboration), planned at the SPS north hall.

Sense wires are stretched coaxially to the chamber, which is 40 cm long and has a 2 mm wire spacing.

Special attention has been placed in minimizing cathode planes support thickness as well as chamber and frames. The total thickness of the prototype is $6 \cdot 10^{-3}$ radiation length. A goal of $2.5 \cdot 10^{-3}$ radiation length could be obtained. A second prototype, with upper and lower cathode printed clockwise and counterclockwise helix-shaped strips, is presently under test.

1. - INTRODUCTION. -

In designing the hadron fragmentation experiment planned at SPS⁽¹⁾, much effort has been devoted to make as compact as possible the detection apparatus surrounding the target.

The general layout of the experiment consist of a forward spectrometer as well as a vertex detector surrounding the target. The forward spectrometer is equipped with drift chambers, scintillator-lead shower detectors and lead glass detectors. It detects particles emitted in a narrow (20 mrad) forward cone. The vertex consist of a set of detectors whose object is to measure the directions of all charged particles and photons emitted at large angles ($5^\circ + 120^\circ$) and to give a first coordinate for tracks which are lost after the first magnet of the forward spectrometer.

(x) - Laboratorio di Cosmogeofisica del CNR - Torino.

2.

Stringent requirements are put forward for designing the vertex detector, i. e. :

- 1) Confinement of the apparatus in a small space region either to limit cost or to fit the small acceptance of the first spectrometer magnet.
- 2) Reduction of the dead space in the detector's frames.
- 3) Compactness of detector outlets (photomultipliers printed circuits, twisted cables) in the region which precedes the target.
- 4) Reduction to a minimum of matter thickness between target and range counters and shower detectors; in order to reduce the effects of multiple scattering and nuclear interactions. This is especially required in the study of the projectile diffraction processes, where the detectable recoil proton momentum must be pushed down to a minimum.

The vertex detector design is shown in Fig. 1. The central core of this apparatus is made of four cylindrical multiwire proportional chambers which the measurement of particle emitted between 30° and 120° is devoted to. The sense wires are stretched parallel to chamber axis; in each chamber upper and lower cathodes are printed in form of helix-shaped strips having for each cathode, a proper angle with respect to the axis. Under condition of moderate event multiplicity each chamber is able to provide a measurement of polar coordinates without ambiguities. Size and tolerance for the set of chambers are given in Table I. A precision of ± 1 mm is required in the processing of induced pulses from cathode strips. In fact the accurate measurement of polar angles is achieved by two following layers of drift

TABLE I

Chamber	Radius (mm)	wires number	Strips number
C ₁	30	90	100
C ₂	60	180	100
C ₃	90	270	100
C ₄	120	360	100

chambers (see Fig. 1), the function of cylindrical chambers being rather of supplying a fast information on the event multiplicity and topology. The vertex detector is completed with 4 scintillator range telescopes, and 12 scintillator - lead shower detector placed around the drift chambers. Furthermore a set of 2 MWPC, 6 drift chambers and a $\bar{\gamma}$ shower detector (± 2.5 mm in precision) is planned in front of the first forward spectrometer magnet.

In this report we describe the construction technique and the results obtained with a first prototype of cylindrical chamber.

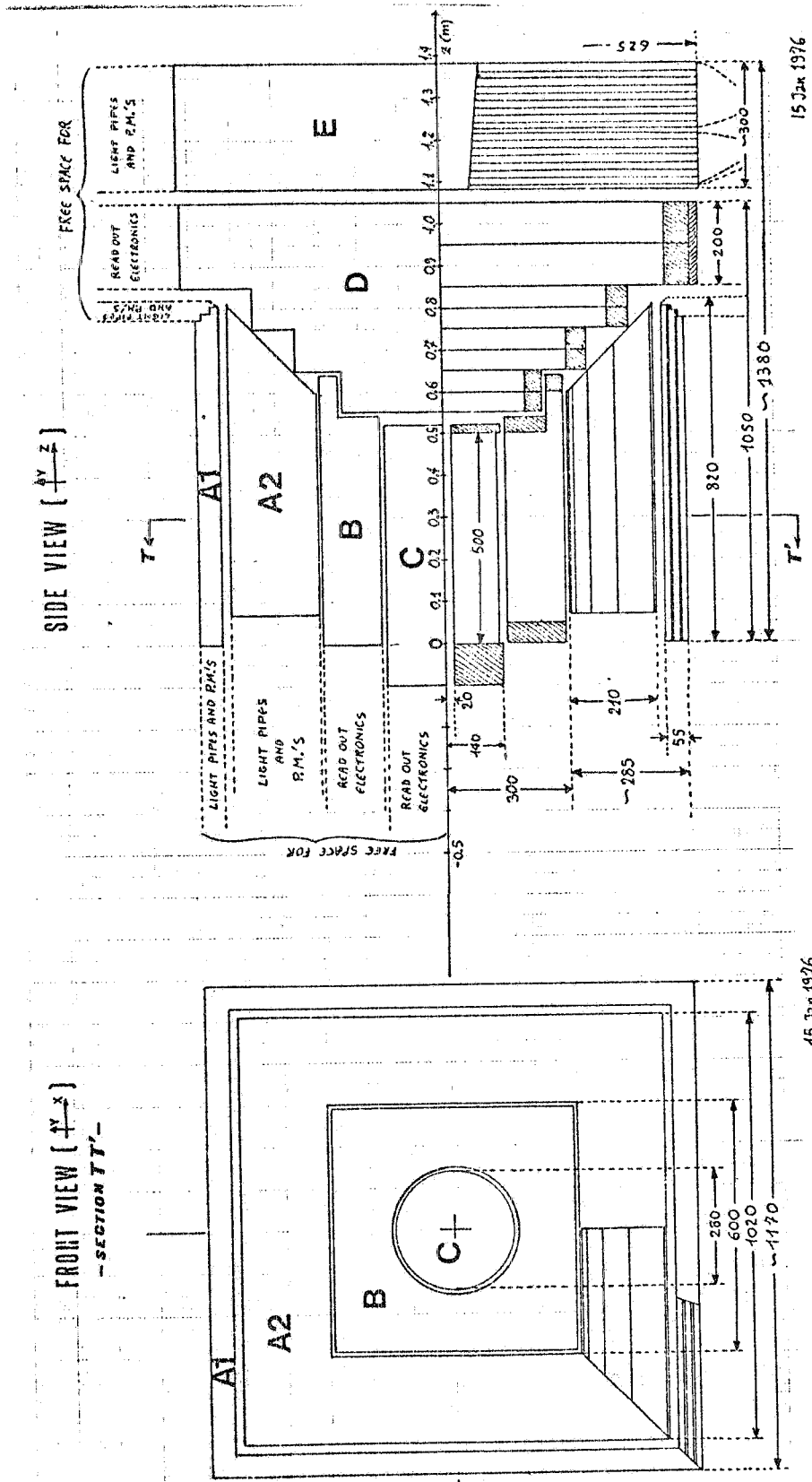


FIG. 1 - Vertex detector structure. Sizes are in mm. A1) Block consists of scintillator + lead shower detectors; A2) Block consist of range counter telescopes; B) Block is a system of drift chambers; C) Block is a system of MWPC; D) Block is a set of 2MWPC and drift planes; E) Is a sandwich of scintillator - lead shower detector, subdivided into 4 set of planes of strips making an angle of 45° to one another.

4.

TABLE II
Rohacell 31

Features of Rohacell 31	Test conditions	Dimension
Density	23°C/50% u. r.	30 Kg/m ³
Tensile strength	23°C/50% u. r.	10 Kp/cm ²
Pressing strength	"	4 "
Flexural strength	"	9 "
Cutting strength	"	4 "
Modulus of elasticity E	"	300 "
Modulus of torsion G	23°C	130 "
Resilience	23°C/50% u. r.	0.4 cm Kp/cm ²
Heat Proofness		200 °C
Thermal conductivity	20°C	113 I/mh°C
H ₂ O Absorption (saturation)	20°C/98% u. r.	0.59 Vol %
H ₂ O Absorption (after 50 days)	20°C (summerged)	18 Vol %
Resistance to organic and propellent solvents	Acetone	resistent
	Ether	"
	Benzol	"
	Methyl alcohol	not resistent
	Sulphuric acid (10%)	"
	Toluol	"
	Soda solution	"

2. - PROTOTYPE CONSTRUCTION TECHNIQUE AND CHARACTERISTICS. -

On grounds of cylindrical MWPC design requirements the major construction difficulty came from the cathode mechanical structure. The right mechanical stiffness and a tolerance of 0.1 mm in electrode distance was required.

The cathode support cylinders has been made by polymethacrylimid plastic foam, whose components are methacrylic acid and methacrylonitrile produced by Rohacell. We used the product Rohacell 31, whose density is 30 Kg/m³. It is characterised by a high resistance to solvents, heating and mechanical actions. The main characteristics are collected in Table II.

Several test have shown that, for a cylinder diameter of 20 cm, a 2 mm thickness of Rohacell 31 is sufficient to ensure the required precision. For a 5 cm diameter, a thickness of 1 mm is sufficient. Cathodes are made of thin Cu-plated Kapton layers (75 μ m Kapton+35 μ m Cu). For the construction of the outer tube of the chamber we adopted the following procedure. The Kapton layer was rolled on a metal cylinder well rectified at the desired diameter (corresponding to the diameter of the outer cathode), with the copper on the side of the cylinder. The plastic foam layer was glued with Araldite on the Kapton. The plastic foam cylinder was rectified and then covered with 25 μ m thick, external protective Kapton sheet glued on it. For the inner tube construction the procedure was analogous, but we begun from the external protection Kapton sheet rolled around the metal cylinder, then covered it by the plastic foam and finally covered by the laminated Kapton with the copper on the outside face. A conservative choice has been made for the first prototype, involving a plastic foam support thickness of 3 mm and no cathode strips. The total thickness of the two shells is thus 0.120g/cm², equivalent to 6.10⁻³ radiation length. The characteristics of the prototype chamber (Fig. 2) are:

external diameter	134 mm
length	400 mm
sense wire spacing	2.1 mm
cathode gap	7 mm

The 20 μ m gold-plated tungsten wires are stretched to 60 g (wire breaks at 90 g). A system of pulleys and weights permitted a stretching uniformity within 1%.

Vetronite frames, equipped with O-rings and mylar guard strips, support the chamber at its ends. High voltage connections, gas inlet and outlet as well as printed circuit for wire connection are collected on a single frame as in the final version the frame which would be placed after the target will be removed. The whole set of chambers will be supported by thin rods and spacers among gaps.

6.

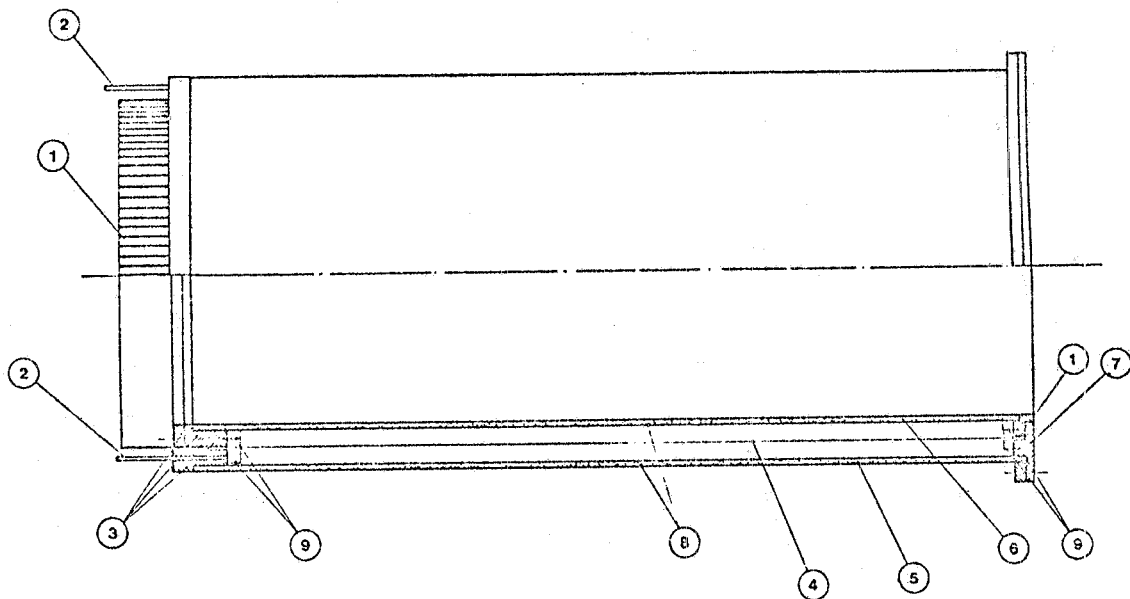


FIG. 2 - Longitudinal cross section of cylindrical chamber prototype:
1) Printed circuit for wires; 2) Gas input; 3) Closure rings; 4) Wires;
5) Rohacell; 6) Rohacell; 7) Closure ring; 8) Cu plated Kapton;
9) Mylar rings.

3. - LABORATORY TEST. -

3.1. - Electronic chain. -

To process the signals from the sense wires we use the electronic chain described in ref. (2). The pulses are sent to a 16-channels preamplifier by means of 10 cm flat multiwire cable, one push-pull output section of a Motorola MC-1035 (with 1.8 k Ω input impedance) being used for each channel. The differential output is transported by twisted pair cables over a distance of 1 m to the processing chain (receiver-trigger-memory module, proportional system encoder and control unit).

The resulting input threshold is about 2.5 mV. Much care was devoted to a proper grounding so that the cross talk between adjacent channels, measured by applying a voltage pulse 50 ns wide to the inputs of the preamplifiers, was 35 db.

In laboratory test data acquisition is performed by a printer which generates, together with the external trigger, the proper read-out commands to control the action of the system encoder.

3.2. - Chamber operation and performance. -

The β particles from a well collimated ($\phi = 1.1$ mm) source (^{90}Sr) were detected in a two scintillation counter telescope (4×30 mm 2 and

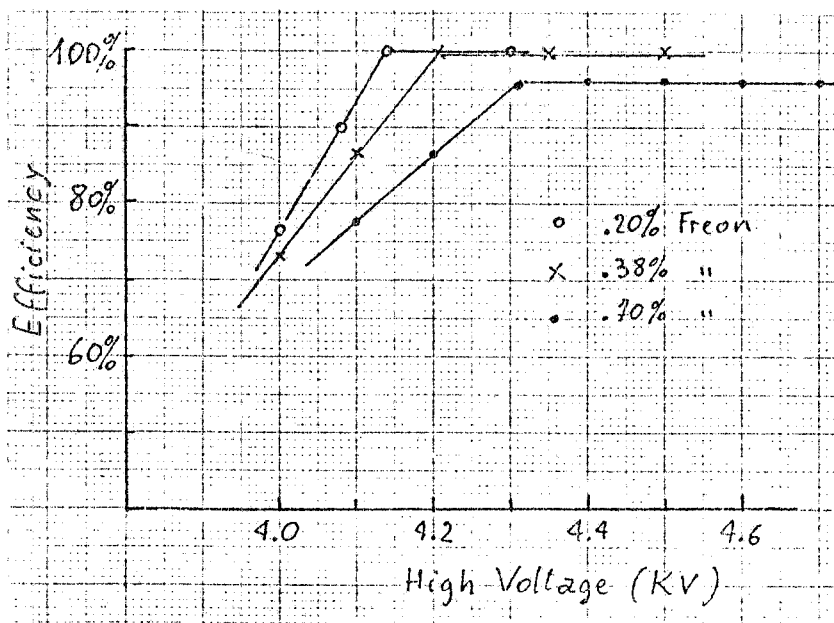


FIG. 3 - Plateau curves for three different concentrations of freon.

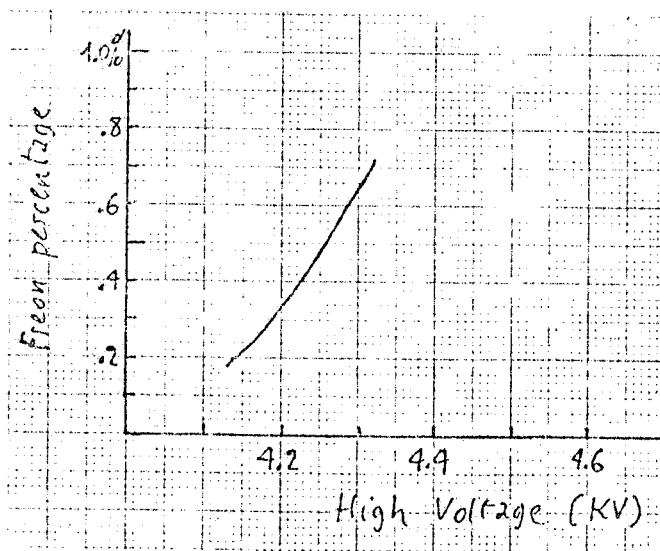


FIG. 4 - Beginning the high-voltage plateau as a function of freon concentration.

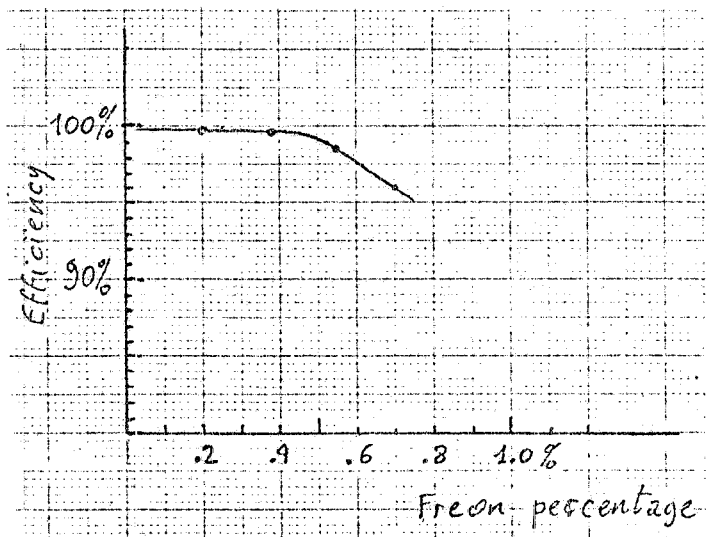


FIG. 5 - Efficiency in the plateau as a function of freon concentration.

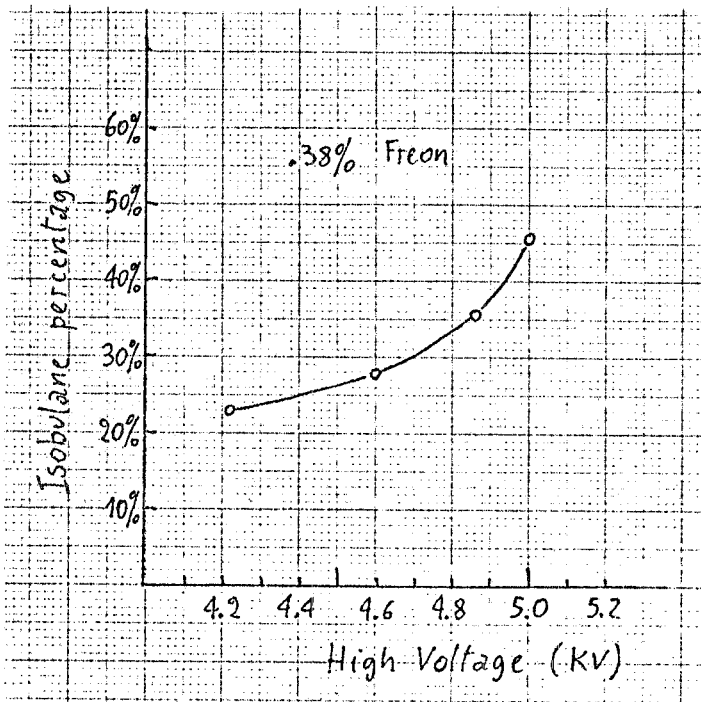


FIG. 6 - Beginning of the high-voltage plateau as a function of isobutane concentration.

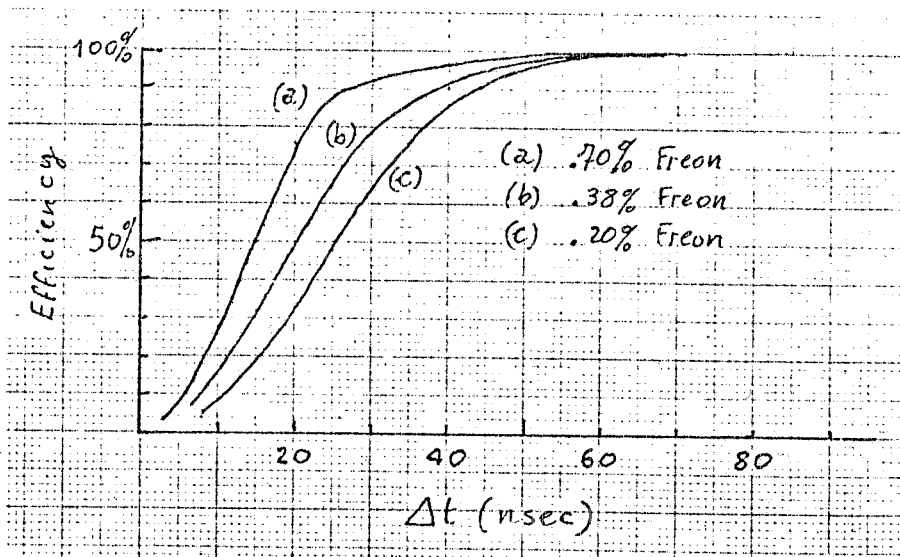
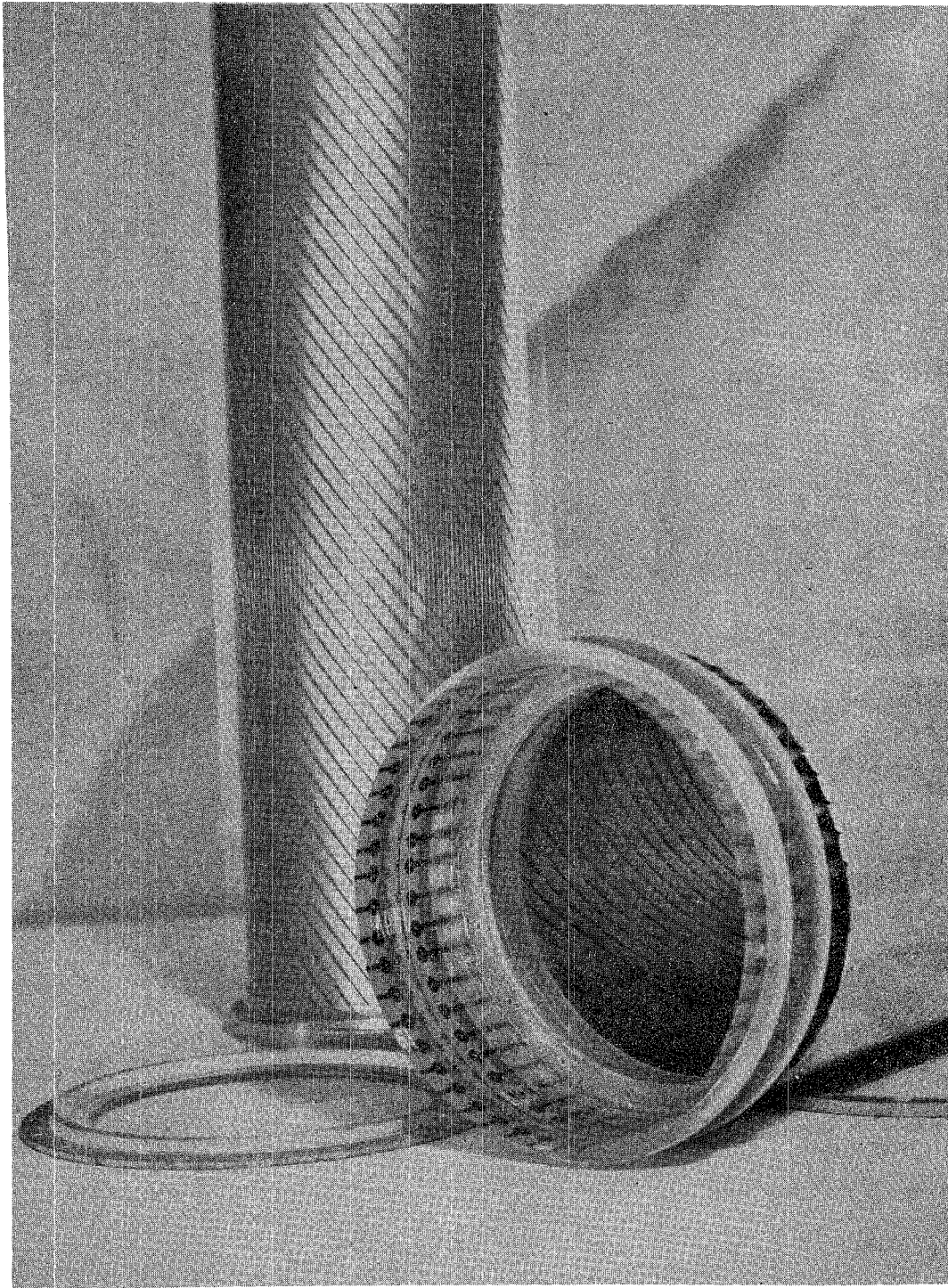


FIG. 7 - Efficiency curve as a function of time resolution.



- FIG. 8 - The two cylinders which constitute the prototype presently under test. Helix-strips as well as sense wires soldered to a printed circuit, which is glued to internal cylinder vetronyte frame, are visible.

$20 \times 30 \text{ mm}^2$) after they passed the chamber. In this arrangement the maximum angle of incidence projected on a plane orthogonal to the wires plane, neglecting multiple scattering, is 0.52 degrees. The particle track is defined in the same plane within about 1.4 mm. Since our analysis is carried out in a group of 32 wires no geometrical limitations in the efficiency measurements result.

Before setting the chamber in operation, sense wires and high voltage electrodes have been cleaned sequentially with amylacetate, methylketone, ethyl alcohol, and liquid freon. The chamber was flushed with a magic gas mixture (argon + isobutane + freon 13 B 1) at a flow rate of $25 \text{ cm}^3/\text{min}$.

After a long term conditioning, during which large background currents and discharges at moderate supply voltage were produced, the chamber regularly improved until a $\lesssim 5 \mu\text{A}$ noise level, summed on all wires, was reached.

3.3. - Plateau curves. -

The efficiency of the chamber was measured by the ratio of the fast OR-pulses which were in coincidence with a 150 ns wide gate generated by the scintillator coincidence and the coincidence counts themselves. The plateau curves for a group of 32 wires as a function of concentrations of freon are reported in Fig. 3. The end of the plateau corresponds to a noise of about 10 Hz/wire with a resulting length of about $250 \div 400 \text{ V}$.

The argon and isobutane concentrations were 76% and 23% respectively. We show in Fig. 4 the beginning of the plateau as a function of freon concentration and in Fig. 5 the efficiency in the plateau. We notice the efficiency drop below 100% for freon concentration larger than 0.38%.

The same measurements have been done by varying the amount of isobutane for a fixed, 0.38%, freon concentration. We present in Fig. 6 the dependence on the isobutane concentration of the beginning of the plateau.

The plateau curves obtained working on others groups of 32 wires coincide within 20 V.

3.4. - Pulse jitter. -

We have measured the time of the fast-or-pulses with respect to the scintillator coincidence with a time-to-amplitude converter.

From the analysis of the time spectra we obtain the efficiency curves normalized to the chamber counts as a function of the gate width plotted in Fig. 7. Irrespective of the freon concentration the full efficiency can be achieved with a gate width at least 70 ns.

The measurements were performed at a high voltage of 30 V after the beginning of the plateau, according to the freon concentration.

10.

3.5. - Multiple-wire firing. -

We have studied the mean wires multiplicity at normal incidence. Source position was chosen with micro displacement to maximize electron flux on the considered wire. Table III gives the percentage of adjacent wires hit for two different cases of freon concentration, working 50 Volt after the beginning of the plateau.

TABLE III

Number of wires counting	Percent	
	.35% F	.8% F
1	90	95%
2	8.5%	5%
3	1.5%	0

All measurements were performed with a 150 ns gate width.

4. - FINAL REMARKS. -

Although tests are not yet completed (a test beam run will be soon performed), we believe that the results obtained with the present prototype are sufficient to ensure cylindrical chamber system facility.

A second chamber is presently under laboratory test with a complete read-out system for sense wires as well for cathode strips. Its sizes are those of the IIIrd chamber in the core of the vertex detector (see Table I).

The components of the chamber are shown in Fig. 8. A further lightening of the chamber, without degradation of mechanical stiffness, is obtainable by using 25 μm thick Kapton cathodes with 17 μm thick copper plating, today commercially available.

In this way a thickness of only $2.5 \cdot 10^{-3}$ radiation length, for particle orthogonal incidence should be obtainable.

REFERENCES. -

- (1) - Amendolia et al., LNF-74/7 (1974) and CERN/SPSC/74/15 (1974);
Amendolia et al., LNF-74/51 (1974) and CERN/SPSC/74-83/P6 (1974).
- (2) - J. Lindsay, Cl. Millezin, J. Cl. Tarlé, H. Verwey and H. Wendler
CERN 74-12 (1974).